Imaging *in vivo*: watching the brain in action

*Jason N. D. Kerr**‡ *and Winfried Denk*‡

Abstract | The appeal of *in vivo* cellular imaging to any neuroscientist is not hard to understand: it is almost impossible to isolate individual neurons while keeping them and their complex interactions with surrounding tissue intact. These interactions lead to the complex network dynamics that underlie neural computation which, in turn, forms the basis of cognition, perception and consciousness. *In vivo* imaging allows the study of both form and function in reasonably intact preparations, often with subcellular spatial resolution, a time resolution of milliseconds and a purview of months. Recently, the limits of what can be achieved *in vivo* have been pushed into terrain that was previously only accessible *in vitro*, due to advances in both physical-imaging technology and the design of molecular contrast agents.

In vivo imaging is, of course, nothing new in biology: it dates back to the very beginnings of microscopy. Examples of this early work are the studies by van Leeuwenhoek[1] and the observation of Brownian motion[2]. However, imaging with high resolution in the living animal while extracting quantitative information has only come to fruition relatively recently, with the development of new imaging methods such as magnetic resonance (MRT; for example, see REF. 3), positron emission (PET; for a review see REF. 4), X-ray (for example, see REF. 5) and optical coherence[6] tomographies, and of nonlinear optical imaging[7]. Although each of these techniques offers insights into neural structure and, in some cases, function, only multi-photon microscopy[7] (MPM) is currently able to resolve the activity and structure of single neurons. This Review will, therefore, focus almost entirely on MPM and its applications to *in vivo* imaging of neural activity and morphology.

The properties of MPM[8–11], which is almost always practiced as two-photon microscopy, make it particularly well suited to deep-tissue imaging. Its application to a whole range of neurobiological challenges, from imaging the activity of neuronal populations to following changes in neurite morphology, is, therefore, not surprising. This has been facilitated by the rise of commercially available systems that make MPM more accessible to biologists. There has been an abundance of reviews describing both the technique and its application to the *in vivo* situation[8,10,12–14], some of them published only recently[11,15–17]. With this in mind, we focus here on how MPM is being used to address questions about neural activity (electrical, chemical and morphological) *in vivo* on timescales ranging from milliseconds[18–20] to months[17,21–29].

MPM is being intensively applied to questions regarding ongoing[30,31] and evoked[32–35] neuronal-population activity. Compared with multi-electrode recording[36,37] (for a review see REF. 38), optical population recording has the advantage that all of the cells in a field of view can be probed, regardless of whether or not they are firing action potentials (APs)[31]. Furthermore, because their spatial locations are precisely known, the cell types of all recorded cells can be determined — if not necessarily *in vivo*, then almost certainly post mortem using immunohistochemical techniques. Imaging is also potentially much less invasive than electrode recording, because light penetrates brain tissue without mechanical disturbance. In addition, because optically recorded neurons are readily identified, MPM can record from the same neurons or their substructures repeatedly over many days and weeks — something that is impossible with electrodes.

In this Review we briefly describe the physical principles of the optical methods behind current *in vivo* imaging, with a focus on MPM. We then discuss key applications of MPM: the imaging of neuronal activity in the single neuron, in subcellular compartments and in neuronal populations; and, finally, the observation and quantification of the morphological stability and plasticity of subcellular neuronal processes.

Principles of *in vivo* optical-imaging methods

The use of light in and near the visible wavelength range (approximately 300–1,100 nm) is the oldest and still most widely applied *in vivo* imaging technique. The resolution

*Network Imaging Group, Max Planck Institute for Biological Cybernetics, Spemannstrasse 41, D-72076 Tuebingen, Germany.
‡Department of Biomedical Optics, Max Planck Institute for Medical Research, Jahnstrasse 29, D-69120 Heidelberg, Germany.
e-mails: jason@tuebingen.mpg.de; denk@mpimf-heidelberg.mpg.de
doi:10.1038/nrn2338
Published online
13 February 2008

Scattering
The deflection of light by particles with a deviating refractive index.

Refractive index
A property of materials that governs the speed of light as it travels through the material and the deflection of light as it crosses boundaries between materials.

Molecular absorption
A process by which the energy of a photon is used to elevate a molecule to a higher internal energy level. The photon itself is eliminated.

Fluorescence
The emission of a photon by a molecule while the molecule undergoes a transition from an elevated energy state to a lower energy state.

Photodamage
The alteration or destruction of biological molecules as a result of photo-oxidative side effects of chromophore excitation.

Signal-to-noise ratio
The ratio between signal size and measurement noise.

High-resistance (sharp) micro electrode
A glass pipette with a tip diameter of less than 100 nm that is filled with saline and used to penetrate cells to gain electrical access to the cell interior.

Tight-seal electrodes
Patch pipettes that are sealed to the plasma membrane and used to carry out electrical recording of the intra-cellular voltage.

Functional MRI
(fMRI). The detection of changes in regional brain activity through their effects on blood flow and blood oxygenation which, in turn, affect the brightness of magnetic-resonance images.

that can be achieved with this method is ultimately determined by the wavelength (but see REF. 39) of the light that is used, but it can be severely degraded by scattering and optical aberrations. For contrast, light microscopy depends on variations in refractive index, molecular absorption or fluorescence properties in the object that is being examined. For *in vivo* imaging, in most cases the detector and the illuminator are located on the same side of the sample (the episcopic configuration), and they often share an objective lens. This precludes the use of most refractive-index-based (phase-contrast) techniques and many absorption-based techniques, which require the detection of transmitted light. The episcopic configuration does allow the use of reflection contrast, in which the signal intensity is determined by a combination of tissue scattering and absorption properties[40–42]. Another technique, optical coherence tomography[43], in which light is selected by interference according to its travel time, allows the depth-resolved imaging of back-scattering properties with high resolution deep inside tissue. Among scattering techniques one should also include harmonic generation[44]. In this technique, owing to the fact that the movement of electrons in a molecule becomes nonlinear at very high instantaneous light intensities, light is generated that has a higher frequency (and hence a smaller wavelength) than the incoming light[45]. Like fluorescence, but unlike ordinary scattering, harmonic generation can be chromophore-specific.

Fluorescence imaging is probably the contrast method that is most widely used for the generation of actual optical-microscopy data. It is almost always performed in the episcopic configuration and is arguably the most versatile contrast technique. This is mostly because of its unrivalled chemical specificity, which results from its multi-stage selectivity: the excitation spectrum, the fluorescence quantum efficiency and the emission spectrum are all specific for the particular fluorophore that is used. Fluorescence (and also back-scattering) contrast can be combined with confocal microscopy[46]. Confocal microscopy can provide optical sectioning (in which information is selectively obtained from a thin slice of the sample) and high resolution, even in tissue that causes a high degree of scattering. However, this comes at the expense of signal size, as most of the fluorescence that comes from the focus is scattered and thus cannot pass through the detector pinhole[47]. The need to increase the excitation power to compensate for this loss then leads to increased photodamage at and around the focus site. This dilemma can be avoided by the use of multi-photon excitation, which relies on the simultaneous absorption of multiple photons and thus depends steeply on the photon concentration (that is, the light intensity)[7,10,48]. As a result, the volume of tissue that is excited is sufficiently confined to obviate the need for spatially resolved detection. This allows the inclusion of scattered fluorescence light[8] and, owing to a lack of excitation, there is no out-of-focus photodamage. Although out-of-focus excitation can also be eliminated by using selective plane illumination[49–51], this technique, unlike MPM, requires transparent specimens and lateral access, neither of which is available in the *in vivo* brain.

In fluorescence microscopy, detector or illumination noise is rarely important; usually the signal-to-noise ratio is limited by photon-shot noise caused by the random arrival of photons at the detector. In particular, for time series (the acquisition of multiple images from the same area, often in rapid succession) it is necessary to obtain as many images as possible using an excitation dose that does not damage the specimen. A high fluorescence-detection efficiency is, therefore, even more essential for *in vivo* opto-physiology than for morphological imaging.

Measuring *in vivo* activity

Although most of our understanding of single-cell physiology has been obtained by studying neurons in varying degrees of isolation, it has long been realized that these findings will have to be placed in the context of natural physiological activity. This can only be achieved by measuring the activity of single neurons *in vivo* (both in the awake and in the anaesthetized state) in order to establish how neurons behave while embedded in intact, active networks. This need has driven the development of *in vivo* electrophysiology techniques that allow the recording of sub-threshold membrane-voltage fluctuations in neurons using high-resistance[52–54] and tight-seal[55–57] electrodes. These developments have included the construction of devices that allow active stabilization of the electrode position[58]. Particularly impressive are recent studies that have mastered whole-cell recording in awake, head-fixed[59] and in freely behaving[60] animals. Under these conditions, modulations of cellular response properties occur that depend on ongoing network activity and are absent *in vitro,* such as network-driven concerted membrane-potential fluctuations[61,62] (up states and down states).

To study network dynamics proper, rather than just the effects of networks on single-cell behaviour, techniques that allow recordings to be made from multiple cells simultaneously are needed. Suitable techniques, such as multiple whole-cell recordings[63–65] or wide-field population imaging[66] with cellular resolution, are available for acute brain slices but are not readily applicable *in vivo*. The imaging of changes in the intrinsic reflectivity of the brain surface[42] and of voltage-sensitive-dye (VSD) fluorescence[67,68] has, for example, shown that ongoing activity *in vivo* can contain spatiotemporal patterns that resemble those that are evoked by external stimuli[69,70] (but see REF. 71). Imaging results are generally consistent with those from electrophysiological experiments[72]. Wide-field imaging of the cortical surface offers millisecond-scale temporal resolution (when using VSDs[73], but not when using the intrinsic, blood-flow-related signal) and can easily be combined with field-potential[74,75] or whole-cell recordings[72]. However, like functional MRI (fMRI), *in vivo* wide-field imaging suffers from low resolution[76]. In this respect, recent results (B. Kuhn, W.D. and R. Bruno, unpublished observations) that were obtained using MPM and a new class of more sensitive[77,78] VSDs *in vivo* are encouraging. In the

following sections we describe some applications of *in vivo* MPM imaging that have begun to shed light on aspects of neuronal function.

Imaging dendritic integration. Following the demonstration that MPM can optically reach depths of several hundred micrometres into the cortex *in vivo*[8], MPM was used to map activity in the dendrites of single neurons, which were filled with a Ca^{2+} indicator through a recording electrode[20]. This allowed dendritic signalling to be studied *in vivo*. One question that has been studied using MPM both in the cortex[18,19,79,80] and in the olfactory bulb[81] is whether the propagation of somatic APs back into the dendritic tree (backpropagation), which appears to be a common requirement for synaptic memory mechanisms and has been studied extensively in brain slices (for a review see REF. 82), also occurs *in vivo*, under conditions of ongoing network activity and the ensuing persistent barrage of synaptic input.

With MPM it was found that in anaesthetized animals, regardless of whether the layer 2/3 cortical pyramidal cells under study were filled and recorded

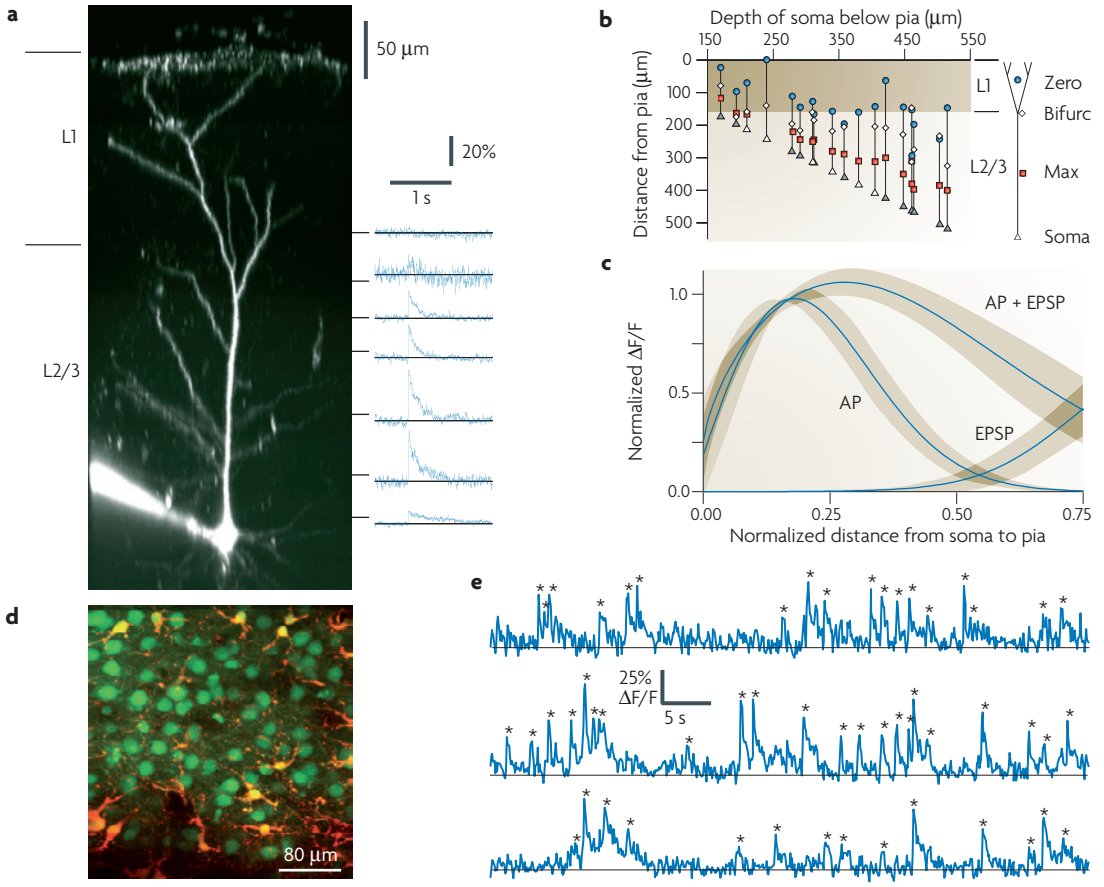

Figure 1 | **Measuring Ca^{2+} transients from dendrites and neuronal populations *in vivo*. a** | On the left is a side projection of a two-photon image stack showing a layer 2/3 (L2/3) pyramidal neuron filled with a Ca^{2+} indicator (Oregon Green BAPTA-1; 200 µM) *in vivo* (the soma was 400 µm from the pia). To the right of this image are Ca^{2+} transients (averaged over 3–5 trials) that were evoked by single action potentials (APs) at the positions indicated along the dendrite. **b** | A schematic representation of neuronal Ca^{2+} transients that were evoked by single APs *in vitro* (filled triangles) and *in vivo* (white triangles). The neurons were ranked according to the depth of their somata below the pial surface. Each neuron is represented as a column of four points (connected by a line). These points represent the depths of the soma (triangle), the bifurcation (bifurc; diamond), the position at which the Ca^{2+} transient was largest (red square) and the position above which it was undetectable (blue circle), as schematically illustrated on the right. **c** | Averaged, normalized and smoothed Ca^{2+} transients recorded *in vivo* from four neurons in response to one AP, one EPSP and one AP paired with one EPSP. Note that the amplitude of the Ca^{2+} transients is more than the sum of each stimulation alone when AP backpropagation coincides with EPSP arrival at the dendritic arbour. Together, these plots illustrate that backpropagating APs fail to reach distal dendrites unless they are boosted by coincident synaptic activity. **d**,**e** | Spiking activity can be simultaneously recorded from all neurons in an area. **d** | An image taken at a depth of 300 µm below the pial surface 2 hours after the application of a Ca^{2+} indicator that labels both neurons and astrocytes and an astrocyte-specific label. Note the labelling of layer 2/3 neuronal somata (green) and astrocytes (yellow). **e** | Normalized fluorescence transients recorded simultaneously from multiple neuronal somata. Transients that were presumably evoked by APs or bursts of APs are labelled with asterisks (see BOX 1). Parts **a**–**c** reproduced, with permission, from REF. 80 © (2003) Society for Neuroscience. Part **e** modified, with permission, from REF. 35 © (2007) Society for Neuroscience.

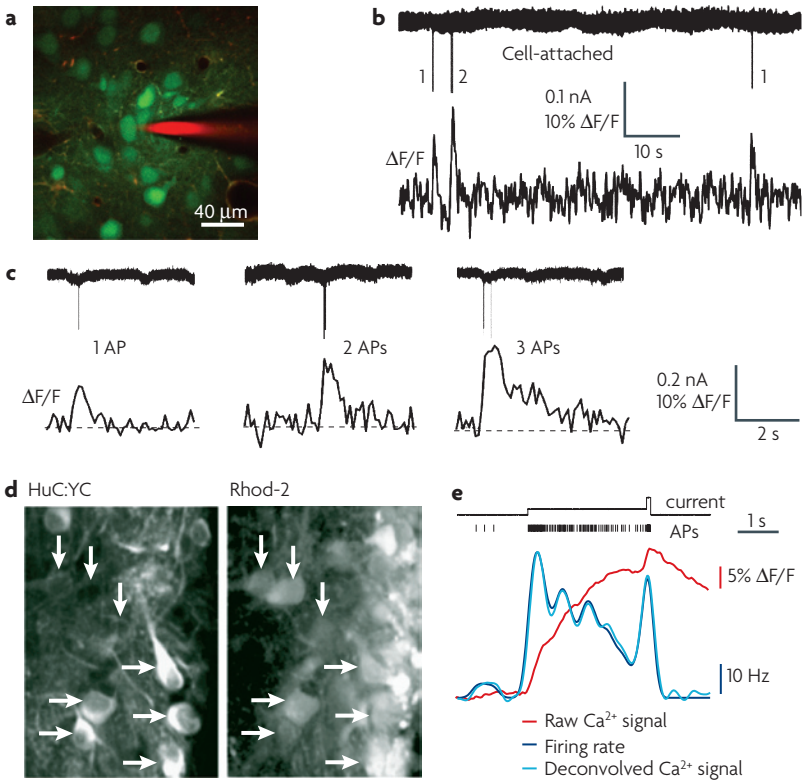

Figure 2 | **Spiking activity in populations of neurons can be inferred from Ca^{2+} transients, with single-action-potential resolution. a** | A glass electrode (red; made visible by including 5 µM Alexa 594 in the filling solution) among a population of neurons (green) and astrocytes (yellow) in the somatosensory cortex. Note the blood vessels surrounded by the astrocytes. **b** | Cell-attached voltage recording (upper trace) and simultaneously recorded somatic Ca^{2+} transients (lower trace) from an experiment similar to the one shown in part **a**. **c** | Examples of Ca^{2+} transients evoked by single (left-hand plot), double (middle plot) and triple (right-hand plot) action potentials (APs) in separate experiments. **d**,**e** | Spike rates can be estimated from the fluorescence signal (F) by deconvolution. Parts **d**,**e** show how this was applied to neurons with high firing rates (5–10 Hz) in zebrafish mitral cells and interneurons[155]. **d** | Fluorescence from expressed HuC:cameleon (labelling mitral cells) (left-hand image) and the ester-trapped Ca^{2+} indicator Rhod-2 (right-hand image) for a field of neurons. The arrows point to eight individual neuronal somata. **e** | From top to bottom: current that was injected into a single neuron, the resultant APs, the resultant Ca^{2+} transient (red trace), a firing-rate estimate (light-blue trace) and the actual firing rate (dark-blue trace). Parts **a**–**c** reproduced, with permission, from REF. 31 © (2005) National Academy of Sciences. Parts **d** and **e** modified, with permission, from REF. 155 © (2006) Macmillan Publishers Ltd.

through high-resistance microelectrodes[19] or in tight-seal mode[80], single-AP-evoked transient increases in Ca^{2+} concentration ($[Ca^{2+}]$) were strong in proximal dendrites but absent in distal dendrites, unless the AP was paired with synaptic stimulation[80] (FIG. 1) or was coincident with ongoing synaptic input[79]. Supralinearity of distant Ca^{2+} transients (in which transients for the combined stimulation are larger than the sum of transients for either stimulation alone) was more pronounced with tight-seal recordings[80].

Discrepancies between dendritic electrical recordings that were carried out using high-resistance electrodes and those that were carried out in the tight-seal mode[19,79,80] highlight how useful it would be to have an optical membrane-voltage probe with a better signal-to-noise ratio than those that are currently available. The use of optical recording would avoid the perils of physical membrane damage by high-resistance microelectrodes and washout of soluble endogenous molecules in the whole-cell mode, which can change dendritic behaviour substantially (as has been shown, for example, in retinal interneurons[83]). Whether backpropagation *in vivo* always resembles the *in vitro* behaviour, or whether it depends, for example, on attention or arousal[79], will ultimately need to be resolved by imaging in awake, behaving animals using either a head-fixed configuration[84] or a head-mounted MP microscope[85–88].

Whenever single cells or specific populations can be labelled with indicators, optical fibres in combination with one-photon techniques[89] can be used to achieve some measure of discrimination between dendritic compartments[90]. In some non-vertebrate species, imaging dendrites *in vivo* with both one- and multi-photon excitation has provided important information that helps us to understand computational processes[91–93].

Imaging population activity. Loading an individual cell with dye does not allow the imaging of activity in multiple cells, let alone in whole populations. What made the imaging of population activity possible in the mammalian brain was not, as in non-mammalian species[94–97], the application of fluorescent Ca^{2+}-indicator proteins (FCIPs)[98]. Instead, it was the adaptation[30] of the ester-trapping technique[99] (FIG. 1d), which is based on creating a membrane-permeable form of the indicator that is converted into a charged and hence impermeable form by endogenous enzymes — a technique that has been successfully used for many years in cell culture and brain slices[66,100]. A number of laboratories seized this opportunity and began using MPM to image the activity of neuron populations in areas in which other bulk-loading techniques had previously been used to map input patterns with wide-field microscopy[101,102]. These included the somatosensory cortex in rats and mice[35,103], the cerebellum in rats[104], the visual cortex in rats, cats[32,33] and mice[34], the tectum in zebrafish[105] and the olfactory bulb in mice[106] and zebrafish[107,108].

In the cat visual cortex, the arrangement of orientation-selective regions in pinwheel patterns was discovered using wide-field *in vivo* optical imaging[109]. With MPM it became possible to resolve the tuning properties of individual cells, and this was used to show that there are sharp boundaries between regions of neurons with different orientation preferences[33]. Again, the imaging results were consistent with electrophysiological findings. Electrophysiology cannot provide the spatial resolution and cellular morphological identification that MPM can, but it does permit single-AP detection which, until recently[31], was unreliable with imaging (FIG. 2). This issue became pressing when *in vivo* whole-cell[110] and juxtasomal[35,111] electrophysiological recordings showed much lower average firing rates and response probabilities than had previously been assumed to exist. In this

Box 1 | **Inferring spikes from Ca^{2+} signals**

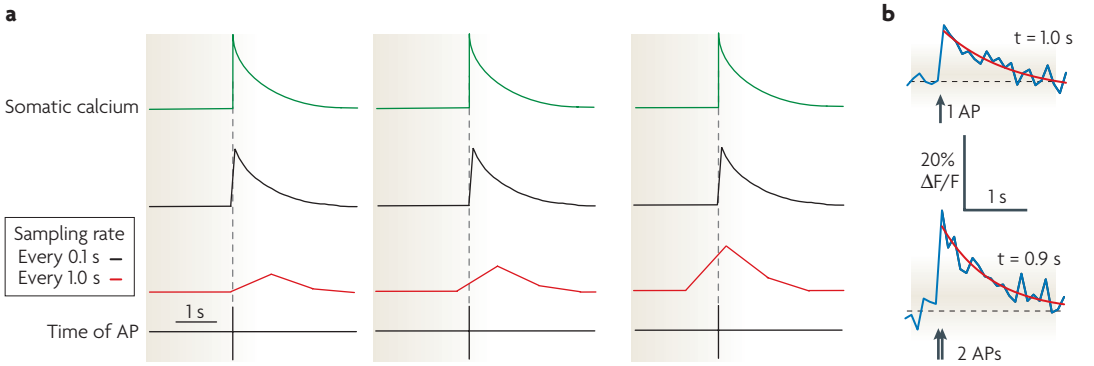

Sample-rate problem

One of the main aims of population imaging is to quantify spiking activity in many neurons simultaneously[31,35,103,155]. In order to achieve this, both single-cell and single-action-potential (AP) resolution are required. If Ca^{2+} transients are to be used to infer spiking activity, then the relationship between the two needs to be established. Detection fidelity can be measured by simultaneous electrical (cell-attached) and Ca^{2+}-transient recording (FIG. 2), as this does not perturb the intracellular contents. To achieve single-AP resolution, the back aperture must be overfilled to avoid contamination by the neuropil signal (BOX 2) and to ensure a high sampling frequency, so that each transient is sampled before it decays into the noise.

In the absence of noise, AP-induced transients can be detected even at low sampling rates (1 sample per second; see figure, part **a**), but the recorded peak amplitudes will vary. For a series of idealized action potentials (bottom trace in part **a** of the figure), sampling at 10 times the decay constant (every 0.1 seconds) reduces such amplitude variations to approximately 10% of peak, allowing the discrimination of single- and double-AP transients, even for moderate signal-to-noise ratios. Part **b** of the figure shows examples of individual Ca^{2+} transients recorded from cortical pyramidal neurons and evoked by a single AP (top) and a two-AP burst (bottom), as indicated by the arrows (these transients were confirmed using cell-attached recordings). Note the fast rise to peak amplitude and the slow exponential decay (illustrated by the red fitted trace). These characteristics mean that for a standard raster scan (which scans at a rate of 1 ms per line), a population of at most approximately 30 neurons can be continually sampled (FIG. 1d). The fast rise allows the precise timing of sufficiently sparse APs to be determined, as the time resolution is limited only by the sampling rate and millisecond precision is possible[114]. The slow decay enables the detection of single-AP-associated signals in bulk-loaded cells during population imaging[31,103] even at slower sampling rates, as long as the firing rates are sufficiently low (which they are in neurons located in the upper cortical layers)[110,111]. Detection reliabilities vary, but they can reach almost 100% in individual neurons[31,35,103]. Although at much higher firing rates single-AP detection is no longer possible, firing rates can be estimated by deconvolution[108] (FIG. 2e). To approach the time resolution that is currently possible with multi-electrode population recordings, improvements in signal-to-noise ratio would be helpful but increased scan speed is paramount. Several approaches to increasing the scan speed are being pursued, including resonant-galvanometer scanning[148] (which increases line frequency but reduces flexibility), targeted scan patterns[162] (in which the beam spends most of its time inside the cells that are to be recorded) and acousto-optical deflection[149] (which requires no moving parts but suffers from severe dispersion issues, as well as a loss in power).

context it is not only important to understand the detection reliability for APs (BOX 1), it is also important to be able to distinguish neuronal somata from glial somata, which fortunately take up some dyes preferentially[112]. Population imaging allows the simultaneous mapping of the receptive fields of many identified cells and, even more importantly, the detection of correlations in neuronal activity[35].

Ester-based loading techniques lead to dense staining (as far as 400 μm from the injection site) of both somata and neurites (FIG. 1), and therefore allow the recording of neuropil activity[31] (BOX 2) but not the attribution of this activity to individual processes. Such attribution is possible when bulk loading is carried out in one region (such as deep in the cortex) and imaging takes place in another region (such as the upper cortex, where the processes of the loaded cells have become sparse and can be individually resolved)[31] (see also REF. 113). It is not yet clear whether it will be possible to detect sub-threshold Ca^{2+} activity in neurites *in vivo*, as is possible *in vitro*[114,115]. Neuropil activity can also contaminate the 'somatic' signal when there is insufficient spatial resolution (BOX 2).

Because of their ability to better target specific cell types, we expect to see increased use of FCIPs in mammals[116–119]. It is possible that these FCIPs will be delivered mainly by viruses, which allow increased expression levels and can deliver the proteins to a wider range of species than transgenic techniques (although they also have disadvantages, such as the potential for damage caused by the injection and by the protein being over-expressed)[120]. Another advantage of FCIPs is that, at least in theory, they allow functional recordings to be carried out in the same cells at multiple points in time — days, weeks and even months apart (see below).

Targeting electrodes. In early imaging studies, dye-filled sharp microelectrodes were driven 'blindly' into the cortex until they successfully penetrated a soma or a dendritic process. Although it is possible to classify

Cell-attached recording
Extracellular electrical recording of a neuron's spiking using a glass patch pipette sealed to the outside of the plasma membrane, without gaining access to the cell interior.

a neuron that has been filled with dye in this manner *post hoc* by imaging its morphology with MPM[20], a bias towards certain cell types (for example, those with large somata) is likely; indeed, some cell types are likely to be missed altogether. More recently, MPM has been used to guide tight-seal recording pipettes towards a fluorescently labelled cell in a process called two-photon targeted patching (TPTP)[121]. Because of the flexibility of sharp electrodes, such targeting can be achieved only in shallow tissue such as the whole-mount retina[122]. In acute slice preparations, optical targeting of neurons with recording electrodes, in this case by infrared differential interference contrast (IR-DIC)[123], allowed patch recordings in brain slices to be made with much greater precision. *In vivo*, TPTP allows recordings to be made from rare fluorescently labelled cells. This has been crucial for establishing spike-detection reliability (BOX 1), and has enabled *in vivo* single-cell genetics studies to be carried out. In these studies, a sparse subset of neurons in an otherwise wild-type brain was infected with a virus[124] that not only changed the physiological properties of the neurons (specifically, their dendritic excitability using RNAi knock-down of a dendrite-specific Na^+-channel subunit) but also labelled them with green fluorescent protein (GFP) and thus permitted testing for changed electrical-response properties by TPTP[125]. The gap between what is possible *in vivo* and *in vitro* has thus narrowed, and single-cell behaviour and network dynamics *in vivo* can now be studied. Where else, aside from in activity measurements, is the *in vivo* context important, and maybe even essential? The issue of whether there is fine-grained structural stability in neurons immediately comes to mind.

Long-term* in vivo *time-lapse imaging. Tissue plasticity and stability are not only central to development (for a review see REF. 126), they might also be important for the acquisition and maintenance of memory in the adult state. Morphological changes during development are substantial and stereotyped and can, therefore, often be detected by post-mortem

Box 2 | **What does bulk-loaded dye report?**

When optically recording from inside the soma of a neuron that has been loaded with a Ca^{2+} indicator, the dominant fluorescent signal is expected to come from the somatic cytosol, as the indicator responds to the Ca^{2+} influx that accompanies action-potential (AP) firing. However, because the trapped dye diffuses freely and thereby fills axons and dendrites (and glial processes) as well as the soma, local neuropil activity can also be recorded. Even though individual axons cannot be resolved, the neuropil signal shows a strong temporal modulation[31]. Moreover, the neuropil signal is highly correlated with both ongoing (sub-threshold) intracellular membrane-potential fluctuations and the electrocorticogram (ECoG), which reports coherent synaptic activity in many cells. For several reasons neuropil Ca^{2+} signals are thought to be mainly axonal in origin. First, locally blocking synaptic transmission does not significantly reduce the Ca^{2+} fluctuations, even though spiking is markedly reduced in local neurons[31]. Second, in bulk-loaded dendrites, transients related to individual APs are observed but fluctuations synchronous with the ECoG are not. Finally, individually filled dendrites show neither sub-threshold Ca^{2+} signals nor backpropagation into distal branches *in vivo*[18,19,80], whereas some of the strongest synchronous neuropil signals are observed in cortical layer 1 (REF. 31).

A clean separation of somatic and neuropil signals cannot be achieved in all cases, and it relies in part on spatial resolution. In particular, imaging with low effective numerical aperture[11,141] (NA) or with wavefront distortions present[143] results in an expanded focal volume. Therefore, faithful recording of somatic signals, which is necessary to reliably detect APs[31,35,103] (BOX 1), might require the use of high-NA lenses and a high effective illumination aperture[141]. In fact, it has been found that an expanded beam entering the objective-lens back aperture (BA; see figure, part **a**) makes AP-evoked Ca^{2+} transients (asterisks in the figure) more distinct in somatic fluorescent signals (see figure, part **b**) by reducing the amount of 'neuropil' contamination (see figure, part **c**) (J.K. and D. Greenberg, unpublished observations). Although such overfilling results in a loss of laser power, the current generation of laser systems supply power in sufficient excess. Overfilling also increases the sensitivity to wavefront aberrations which might need to be corrected using adaptive optics, particularly when imaging through thinned bone[143].

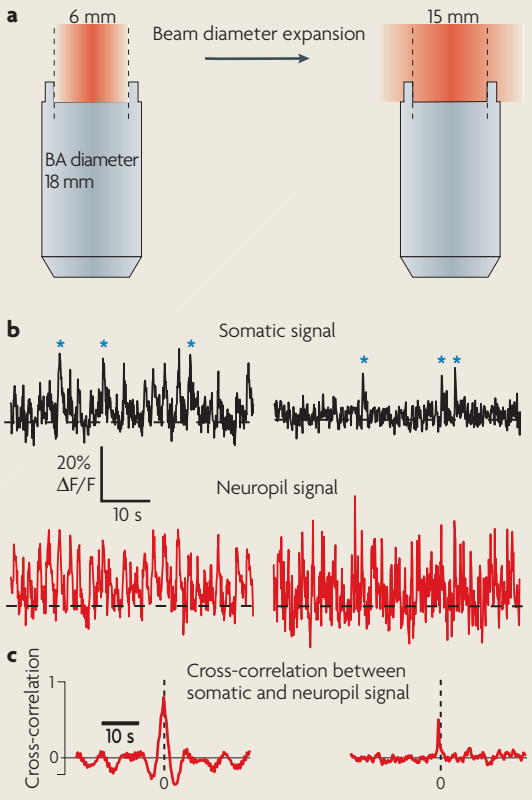

Patch recordings
Electrical recordings made using a glass pipette with a tip diameter of approximately 1 micrometre that is filled with saline and used to form gigaohm seals on the cell membrane. By removing the membrane patch inside the pipette, electrical access to the cell interior can be gained.

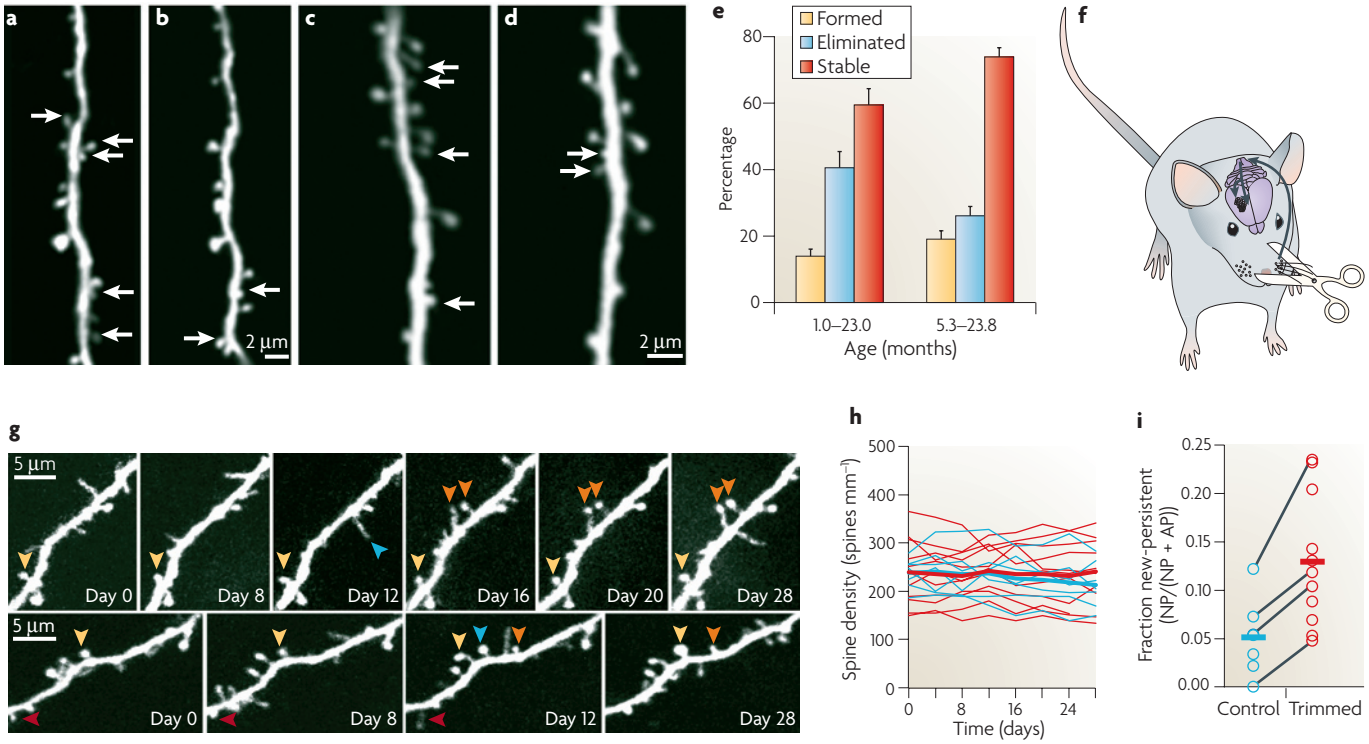

Figure 3 | **The persistence of dendritic spines in adult mice, revealed by *in vivo* imaging. a–d** | Dendritic branches from two animals. For each animal, two images were obtained 18 months apart (animal 1: **a**,**b**; animal 2: **c**,**d**). Note that most of the spines in **a** and **c** persist in **b** and **d**. **e** | The percentage of spines that were eliminated, formed or persistent over 18–22 months. **f–i** | The effects of sensory experience on spine persistence. **f** | Trimming of alternate whiskers generates different sensory experiences for neighbouring whisker barrels. **g** | A high-magnification view of two dendritic segments imaged before (days 0–8) and after (days 12–28) whisker trimming. The arrowheads show spines that were always present (AP; yellow); new persistent spines (NP, orange); lost persistent spines (red); and transient spines (blue). **h** | Spine density does not change significantly over time in control (blue) or deprived (red) locations. **i** | Quantification of NP spines, showing that total numbers of NP spines were a small fraction of the total number of persistent spines and that trimming enhanced this fraction. Every circle represents a cell, and the horizontal bars represent the group averages. Grey lines connect paired experiments. Parts **a–e** reproduced, with permission, from REF. 135 © (2005) Elsevier Science. Parts **g–i** reproduced, with permission, from REF. 136 © (2006) Macmillan Publishers Ltd.

analysis of specimens of different ages (for a review see REF. 127). However, such studies are labour intensive and, more importantly, are fundamentally unable to detect dynamics that leave statistical properties, such as the densities of synapses or the volume fractions that are occupied by axons and dendrites, unaltered. This became clear during the pioneering studies of synapse elimination in the neuromuscular junction, in which the behaviour of individual terminals was followed in time[128,129].

In the mammalian cortex it was unknown whether synaptic contacts, the density of which is constant in the adult[22], change with time and, if so, at what rate. Without a label that is specific for newly formed synapses being available, observation of the same tissue region in the same animal over a period of weeks or months (time-lapse imaging) is needed. Furthermore, unlike a novel-synapse label, such time-lapse imaging also allows the detection and quantification of highly fluctuating intermediate states[27,126,130,131]. In developing embryos, which are often optically transparent, and in the peripheral nervous system (mostly the neuromuscular junction), time-lapse imaging is possible with wide-field or confocal microscopy[128,132,133].

Only in recent years have such experiments become possible in the adult mammalian brain, through the use of MPM combined with cellular labelling and trans-genetically introduced protein-based fluorophores[134]. Retrospective electron microscopy has been used to demonstrate that spines that had been shown by *in vivo* time-lapse imaging to be newly formed contain all of the structural elements that are typical for synapses[24]. All studies have found that there is a high degree of structural stability[135]. Nevertheless, the turnover rates for dendritic spines that have been reported by different laboratories vary by a factor of at least five (see REF. 23 and the references cited therein; FIG. 3). The rates appear to depend on cell type, are affected by the presence or absence of sensory stimulation[26,136], and also seem to depend on the method that is used to gain optical access to the cortex[23]. In particular, the creation of an open-skull window appears to lead to the activation of microglia, which respond rapidly to brain injury[137] and might contribute to higher spine turnover rates. Although axonal-bouton turnover matches spine turnover rates both in rodents[138] and primates[29], these experiments have been carried out with opened skulls and, therefore, some of the issues

that have been encountered in the experiments that measured spine turnover might also apply here.

Integration of newborn neurons into existing circuits has also been observed. First a lentivirus containing the gene for GFP was injected into the subventricular zone, where olfactory receptor neurons are born, and then MPM was used to observe these neurons as they migrated, matured and integrated into the circuit[139]. It might be interesting to use TPTP to test, more directly, the evolution of the physiological properties of these neurons as well as their synaptic integration into the neuronal circuit.

Technical issues

The key advantage of MPM is its ability to image deep in light-scattering tissue[8–10], but the reachable depth is still limited to approximately 1 mm. This is not because of limits in the available laser power, because it is possible to use amplified pulses at a lower repetition rate to boost nonlinear effects[140], but because of substantial two-photon excitation near the sample surface. Even though this surface excitation is spread over a large area, the laser power is undiminished by scattering. The extent of the excitation depends on the numerical aperture of the objective lens and, even more strongly, on the labelling distribution, with more uniform distributions leading to stronger relative background excitation[141]. Imaging depth, resolution and signal size are also affected by distortions of the laser-beam wavefront that are caused by refractive-index heterogeneities in the sample. Such distortions enlarge the focus beyond its diffraction-limited extent but can be pre-empted, if they can be measured[142], by adaptively pre-distorting the wavefront that goes into the sample[143].

Another area in which technological advances have a key role is in imaging awake, behaving animals. Although miniaturized amplifier head stages are now routinely used for the recording of APs from multiple cells (for a review see REF. 144), in awake, freely moving animals similar efforts in optical microscopy [85,145] are still at an experimental stage. Miniaturized objectives and scanners[86,88] have been developed and used in conjunction with fibre-optic excitation-light delivery and fluorescence-light collection to record images from moving animals. Single-position fluorescence signals from moving animals can be recorded using one-photon excitation and detection through a multi-mode optical fibre[89]. An alternative, and very promising, approach is to use a conventional MPM but provide virtual-reality motion for awake, head-fixed animals[84].

What does the future hold for *in vivo* MP imaging?

The issue of dendritic information integration and how it depends on factors such as wakefulness, attention and expectation is likely to become prominent in single-cell *in vivo* imaging. The requisite tools, such fibre-coupled microscopes[85,88,145,146] or head-fixed virtual-reality systems[84], have already been demonstrated. On the axonal side, the modulation (again, by factors such as attention) of residual Ca^{2+}, which is known from *in vitro* studies to influence short-term synaptic plasticity[147], might be an interesting target for investigation *in vivo*. Arguably more important for the understanding of neural computation will, in our view, be the ability to measure population activity with cellular, single-AP and potentially millisecond resolution. Here the fact that MPM is a fundamentally serial technique (parallelization of MPM is possible but, because it requires spatially resolved detection, it comes at the expense of the ability to work deep in strongly scattering tissue) presents a technological challenge if many points in space are to be recorded. This is because the focus has to be moved sufficiently quickly for it to visit all cells or cellular compartments at least once during each unit of temporal resolution. Possible methods for fast in-plane movement are resonant-mirror scanning[148] and acousto–optical deflection[149]. The latter can also be used to shift the focus to some extent along the optical axis[150], which otherwise requires the microscope objective to be moved[151]. The ability to scan in three dimensions will be essential to cover even localized populations completely.

There are many questions, such as what fractions of which cell types are active during a certain behaviour or sensory input, that require not only simultaneous recording from multiple cells, but also the cells' spatial localization and cell-type classification. Increasingly refined genetic labelling techniques will be important for indicating cell type definitively, and combinatorial uses of differently coloured fluorescent proteins will potentially be required[152]. It will be interesting to see whether it will be possible to overcome the current inaccessibility of deeper brain structures while keeping the damage to the penetrated overlying brain structures to an acceptable level by using penetrating imaging devices[146,153,154].

Spiking appears to be represented in a rather linear fashion by increases in $[Ca^{2+}]$ [31,155], but $[Ca^{2+}]$ is a non-linear measure of sub-threshold activity. A method by which to measure the membrane voltage directly would, therefore, be desirable. Even more important might be the measurement of other local biochemical signals and the ability to determine how they are dependent on local activity and its history. Measurements of glial activity have revealed that astrocytes have a role in regulating arterial blood flow[156] and show a rapid increase in $[Ca^{2+}]$ upon sensory stimulation[157].

Imaging is likely to be helpful in understanding how developmental and adult-morphological dynamics are related to each other and, possibly, to memory formation, memory consolidation and mental disease[158]. Models of neurodegenerative disease should benefit greatly from the ability to follow the development of characteristic cellular pathologies, such as tangles and plaques[159,160], and how these pathologies respond to various forms of therapeutic intervention. Even the development of diagnostic tools based on endoscopic MPM is a distinct possibility. Coarser volume-imaging methods, such MRI, could first provide an individualized anatomical reference[161] and then, with the help of functional signals (fMRI and PET), guide the placement of the optical recordings.

Numerical aperture
A measure of the angular spread of the light rays that emerge from or are able to enter an objective lens.

1. Dobell, C. *Antony van Leeuwenhoek and his "Little Animals"* (John Bale, Sons and Danielsson, London, 1932).
2. Brown, R. A brief account of microscopical observations made in the months of June, July and August, 1827, on the particles contained in the pollen of plants; and on the general existence of active molecules in organic and inorganic bodies. *Phil. Mag.* **4**, 161–173 (1828).
3. Callaghan, P. T. *Principles of Nuclear Magnetic Resonance Microscopy* (Clarendon, 1991).
4. Schmidt, K. C. & Smith, C. B. Resolution, sensitivity and precision with autoradiography and small animal positron emission tomography: implications for functional brain imaging in animal research. *Nucl. Med. Biol.* **32**, 719–725 (2005).
5. Romans, L. E. *Introduction to Computed Tomography* (Lippincott, Williams & Wilkins, London, 1995).
6. Fujimoto, J. G. Optical coherence tomography for ultrahigh resolution *in vivo* imaging. *Nature Biotechnol.* **21**, 1361–1367 (2003).
7. Denk, W., Strickler, J. H. & Webb, W. W. Two-photon laser scanning fluorescence microscopy. *Science* **248**, 73–76 (1990).
This study provided the first demonstration that two-photon excitation can be used to image fluorescently stained living cells and cellular substructures.
8. Denk, W. *et al.* Anatomical and functional imaging of neurons using 2-photon laser scanning microscopy. *J. Neurosci. Methods* **54**, 151–162 (1994).
9. Denk, W. Two-photon excitation in functional biological imaging. *J. Biomed. Opt.* **1**, 296–304 (1996).
10. Denk, W. & Svoboda, K. Photon upmanship: why multiphoton imaging is more than a gimmick. *Neuron* **18**, 351–357 (1997).
11. Helmchen, F. & Denk, W. Deep tissue two-photon microscopy. *Nature Methods* **2**, 932–940 (2005).
This reference and reference 10 are important technically orientated reviews of the application of two-photon excitation to neurobiology, and provide a good introduction to the technique for a general readership.
12. Williams, R. M., Piston, D. W. & Webb, W. W. 2-photon molecular-excitation provides intrinsic 3-dimensional resolution for laser-based microscopy and microphotochemistry. *FASEB J.* **8**, 804–813 (1994).
13. Denk, W., Piston, D. W. & Webb, W. W. in *The Handbook of Confocal Microscopy* (ed. Pawley, J.) 445–458 (Plenum, New York, 1995).
14. Zipfel, W. R., Williams, R. M. & Webb, W. W. Nonlinear magic: multiphoton microscopy in the biosciences. *Nature Biotechnol.* **21**, 1368–1376 (2003).
15. Diaspro, A., Chirico, G. & Collini, M. Two-photon fluorescence excitation and related techniques in biological microscopy. *Q. Rev. Biophys.* **38**, 97–166 (2005).
16. Oheim, M., Michael, D. J., Geisbauer, M., Madsen, D. & Chow, R. H. Principles of two-photon excitation fluorescence microscopy and other nonlinear imaging approaches. *Adv. Drug Deliv. Rev.* **58**, 788–808 (2006).
17. Svoboda, K. & Yasuda, R. Principles of two-photon excitation microscopy and its applications to neuroscience. *Neuron* **50**, 823–839 (2006).
18. Helmchen, F., Svoboda, K., Denk, W. & Tank, D. W. *In vivo* dendritic calcium dynamics in deep-layer cortical pyramidal neurons. *Nature Neurosci.* **2**, 989–996 (1999).
19. Svoboda, K., Helmchen, F., Denk, W. & Tank, D. W. Spread of dendritic excitation in layer 2/3 pyramidal neurons in rat barrel cortex *in vivo*. *Nature Neurosci.* **2**, 65–73 (1999).
20. Svoboda, K., Denk, W., Kleinfeld, D. & Tank, D. W. *In vivo* dendritic calcium dynamics in neocortical pyramidal neurons. *Nature* **385**, 161–165 (1997).
21. Grutzendler, J., Kasthuri, N. & Gan, W. B. Long-term dendritic spine stability in the adult cortex. *Nature* **420**, 812–816 (2002).
22. Trachtenberg, J. T. *et al.* Long-term *in vivo* imaging of experience-dependent synaptic plasticity in adult cortex. *Nature* **420**, 788–794 (2002).
This reference and reference 21 used MPM in combination with genetically labelled neurons to follow changes in dendritic spine morphology over many months. This enabled the quantification of spine turnover rates (see also references 23–26 and 135).
23. Xu, H. T., Pan, F., Yang, G. & Gan, W. B. Choice of cranial window type for *in vivo* imaging affects dendritic spine turnover in the cortex. *Nature Neurosci.* **10**, 549–551 (2007).
24. Knott, G. W., Holtmaat, A., Wilbrecht, L., Welker, E. & Svoboda, K. Spine growth precedes synapse formation in the adult neocortex *in vivo*. *Nature Neurosci.* **9**, 1117–1124 (2006).
25. Grutzendler, J. & Gan, W. B. Two-photon imaging of synaptic plasticity and pathology in the living mouse brain. *NeuroRx* **3**, 489–496 (2006).
26. Zuo, Y., Yang, G., Kwon, E. & Gan, W. B. Long-term sensory deprivation prevents dendritic spine loss in primary somatosensory cortex. *Nature* **436**, 261–265 (2005).
27. Portera-Cailliau, C., Weimer, R. M., De Paola, V., Caroni, P. & Svoboda, K. Diverse modes of axon elaboration in the developing neocortex. *PloS Biol.* **3**, 1473–1487 (2005).
28. Holtmaat, A. J. *et al.* Transient and persistent dendritic spines in the neocortex *in vivo*. *Neuron* **45**, 279–291 (2005).
29. Stettler, D. D., Yamahachi, H., Li, W., Denk, W. & Gilbert, C. D. Axons and synaptic boutons are highly dynamic in adult visual cortex. *Neuron* **49**, 877–887 (2006).
30. Stosiek, C., Garaschuk, O., Holthoff, K. & Konnerth, A. *In vivo* two-photon calcium imaging of neuronal networks. *Proc. Natl Acad. Sci. USA* **100**, 7319–7324 (2003).
This was the first study to image Ca^{2+} transients *in vivo* from neuronal populations bulk-loaded with membrane-permeable Ca^{2+}-indicator dyes. Most commercially available Ca^{2+}-indicator dyes were tried.
31. Kerr, J. N., Greenberg, D. & Helmchen, F. Imaging input and output of neocortical networks *in vivo*. *Proc. Natl Acad. Sci. USA* **102**, 14063–14068 (2005).
Using simultaneous imaging and targeted electrical recordings, this study showed that it was possible to infer electrical activity with single-cell and single-AP accuracy from Ca^{2+} transients measured in populations of bulk-loaded neurons (see also references 35, 103 and 155).
32. Ohki, K., Chung, S., Ch'ng, Y. H., Kara, P. & Reid, R. C. Functional imaging with cellular resolution reveals precise micro-architecture in visual cortex. *Nature* **433**, 597–603 (2005).
Using MPM and Ca^{2+} imaging, this study showed that neurons in the cat visual cortex are precisely arranged according to their preferred orientation and direction, but that neurons in the rat visual cortex are not (see also reference 33).
33. Ohki, K. *et al.* Highly ordered arrangement of single neurons in orientation pinwheels. *Nature* **442**, 925–928 (2006).
34. Mrsic-Flogel, T. D. *et al.* Homeostatic regulation of eye-specific responses in visual cortex during ocular dominance plasticity. *Neuron* **54**, 961–972 (2007).
35. Kerr, J. N. *et al.* Spatial organization of neuronal population responses in layer 2/3 of rat barrel cortex. *J. Neurosci.* **27**, 13316–13328 (2007).
36. Gabriel, M. A system for multiple unit recording during avoidance behavior of the rabbit. *Physiol. Behav.* **12**, 145–148 (1974).
37. Kruger, J. & Bach, M. Simultaneous recording with 30 microelectrodes in monkey visual cortex. *Exp. Brain Res.* **41**, 191–194 (1981).
38. Shoham, S., O'Connor D, H. & Segev, R. How silent is the brain: is there a "dark matter" problem in neuroscience? *J. Comp. Physiol. A Neuroethol. Sens. Neural Behav. Physiol.* **192**, 777–784 (2006).
39. Hell, S. W. Far-field optical nanoscopy. *Science* **316**, 1153–1158 (2007).
40. Frostig, R. D., Lieke, E. E., Ts'o, D. Y. & Grinvald, A. Cortical functional architecture and local coupling between neuronal activity and the microcirculation revealed by *in vivo* high-resolution optical imaging of intrinsic signals. *Proc. Natl Acad. Sci. USA* **87**, 6082–6086 (1990).
41. Grinvald, A., Frostig, R. D., Siegel, R. M. & Bartfeld, E. High-resolution optical imaging of functional brain architecture in the awake monkey. *Proc. Natl Acad. Sci. USA* **88**, 11559–11563 (1991).
42. Grinvald, A., Lieke, E., Frostig, R. D., Gilbert, C. D. & Wiesel, T. N. Functional architecture of cortex revealed by optical imaging of intrinsic signals. *Nature* **324**, 361–364 (1986).
43. Huang, D. *et al.* Optical coherence tomography. *Science* **254**, 1178–1181 (1991).
44. Mertz, J. Nonlinear microscopy: new techniques and applications. *Curr. Opin. Neurobiol.* **14**, 610–616 (2004).
45. Franken, P. A. & Ward, J. F. Optical harmonics and nonlinear phenomena. *Rev. Mod. Phys.* **35**, 23–39 (1963).
46. Minsky, M. Microscopy apparatus. US patent 3013467 (1961).
47. Centonze, V. E. & White, J. G. Multiphoton excitation provides optical sections from deeper within scattering specimens than confocal imaging. *Biophys. J.* **75**, 2015–2024 (1998).
48. Squirrell, J. M., Wokosin, D. L., White, J. G. & Bavister, B. D. Long-term two-photon fluorescence imaging of mammalian embryos without compromising viability. *Nature Biotechnol.* **17**, 763–767 (1999).
49. Voie, A. H., Burns, D. H. & Spelman, F. A. Orthogonal-plane fluorescence optical sectioning — 3-dimensional imaging of macroscopic biological specimens. *J. Microsc.* **170**, 229–236 (1993).
50. Voie, A. H. Imaging the intact guinea pig tympanic bulla by orthogonal-plane fluorescence optical sectioning microscopy. *Hear. Res.* **171**, 119–128 (2002).
51. Huisken, J., Swoger, J., Del Bene, F., Wittbrodt, J. & Stelzer, E. H. K. Optical sectioning deep inside live embryos by selective plane illumination microscopy. *Science* **305**, 1007–1009 (2004).
52. Creutzfeldt, O. D., Watanabe, S. & Lux, H. D. Relations between EEG phenomena and potentials of single cortical cells. I. Evoked responses after thalamic and epricortical stimulation. *Electroencephalogr. Clin. Neurophysiol.* **20**, 1–18 (1966).
53. Watanabe, S., Konishi, M. & Creutzfeldt, O. D. Postsynaptic potentials in the cat's visual cortex following electrical stimulation of afferent pathways. *Exp. Brain Res.* **1**, 272–283 (1966).
54. Eccles, J. C., Llinas, R. & Sasaki, K. The excitatory synaptic action of climbing fibres on the Purkinje cells of the cerebellum. *J. Physiol.* **182**, 268–296 (1966).
55. Jagadeesh, B., Gray, C. M. & Ferster, D. Visually evoked oscillations of membrane potential in cells of cat visual cortex. *Science* **257**, 552–554 (1992).
56. Brecht, M. & Sakmann, B. Whisker maps of neuronal subclasses of the rat ventral posterior medial thalamus, identified by whole-cell voltage recording and morphological reconstruction. *J. Physiol.* **538**, 495–515 (2002).
57. Margrie, T. W., Brecht, M. & Sakmann, B. *In vivo*, low-resistance, whole-cell recordings from neurons in the anaesthetized and awake mammalian brain. *Pflugers Arch.* **444**, 491–498 (2002).
58. Fee, M. S. Active stabilization of electrodes for intracellular recording in awake behaving animals. *Neuron* **27**, 461–468 (2000).
59. Crochet, S. & Petersen, C. C. Correlating whisker behavior with membrane potential in barrel cortex of awake mice. *Nature Neurosci.* **9**, 608–610 (2006).
60. Lee, A. K., Manns, I. D., Sakmann, B. & Brecht, M. Whole-cell recordings in freely moving rats. *Neuron* **51**, 399–407 (2006).
61. Wilson, C. J. & Groves, P. M. Spontaneous firing patterns of identified spiny neurons in the rat neostriatum. *Brain Res.* **220**, 67–80 (1981).
62. Wilson, C. J. & Kawaguchi, Y. The origins of two-state spontaneous membrane potential fluctuations of neostriatal spiny neurons. *J. Neurosci.* **16**, 2397–2410 (1996).
63. Markram, H., Lubke, J., Frotscher, M., Roth, A. & Sakmann, B. Physiology and anatomy of synaptic connections between thick tufted pyramidal neurones in the developing rat neocortex. *J. Physiol.* **500**, 409–440 (1997).
64. Magee, J. C. & Johnston, D. A synaptically controlled, associative signal for Hebbian plasticity in hippocampal neurons. *Science* **275**, 209–213 (1997).
65. Larkum, M. E., Zhu, J. J. & Sakmann, B. A new cellular mechanism for coupling inputs arriving at different cortical layers. *Nature* **398**, 338–341 (1999).
66. Cossart, R., Lkegaya, Y. & Yuste, R. Calcium imaging of cortical networks dynamics. *Cell Calcium* **37**, 451–457 (2005).
67. Grinvald, A., Anglister, L., Freeman, J. A., Hildesheim, R. & Manker, A. Real-time optical imaging of naturally evoked electrical activity in intact frog brain. *Nature* **308**, 848–850 (1984).
68. Shoham, D. *et al.* Imaging cortical dynamics at high spatial and temporal resolution with novel blue voltage-sensitive dyes. *Neuron* **24**, 791–802 (1999).
This paper, together with reference 67, described the use of voltage-sensitive dyes for imaging activity from large areas of the cortex in both awake and anaesthetized animals. The approach was then complemented with simultaneous electrical recordings (see reference 69).

69. Arieli, A., Sterkin, A., Grinvald, A. & Aertsen, A. Dynamics of ongoing activity: explanation of the large variability in evoked cortical responses. *Science* **273**, 1868–1871 (1996).
70. Kenet, T., Bibitchkov, D., Tsodyks, M., Grinvald, A. & Arieli, A. Spontaneously emerging cortical representations of visual attributes. *Nature* **425**, 954–956 (2003).
71. Xu, W., Huang, X., Takagaki, K. & Wu, J. Y. Compression and reflection of visually evoked cortical waves. *Neuron* **55**, 119–129 (2007).
72. Petersen, C. C., Grinvald, A. & Sakmann, B. Spatiotemporal dynamics of sensory responses in layer 2/3 of rat barrel cortex measured *in vivo* by voltage-sensitive dye imaging combined with whole-cell voltage recordings and neuron reconstructions. *J. Neurosci.* **23**, 1298–1309 (2003).
73. Grinvald, A. & Hildesheim, R. VSDI: a new era in functional imaging of cortical dynamics. *Nature Rev. Neurosci.* **5**, 874–885 (2004).
74. Arieli, A. & Grinvald, A. Optical imaging combined with targeted electrical recordings, microstimulation, or tracer injections. *J. Neurosci. Methods* **116**, 15–28 (2002).
75. Civillico, E. F. & Contreras, D. Comparison of responses to electrical stimulation and whisker deflection using two different voltage-sensitive dyes in mouse barrel cortex *in vivo*. *J. Membr. Biol.* **208**, 171–182 (2005).
76. Ogawa, S. *et al.* intrinsic signal changes accompanying sensory stimulation — functional brain mapping with magnetic-resonance-imaging. *Proc. Natl Acad. Sci. USA* **89**, 5951–5955 (1992).
77. Hubener, G., Lambacher, A. & Fromherz, P. Anellated hemicyanine dyes with large symmetrical solvatochromism of absorption and fluorescence. *J. Phys. Chem. B* **107**, 7896–7902 (2003).
78. Kuhn, B., Fromherz, P. & Denk, W. High sensitivity of Stark-shift voltage-sensing dyes by one- or two-photon excitation near the red spectral edge. *Biophys. J.* **87**, 631–639 (2004).
79. Waters, J. & Helmchen, F. Boosting of action potential backpropagation by neocortical network activity *in vivo*. *J. Neurosci.* **24**, 11127–11136 (2004).
80. Waters, J., Larkum, M., Sakmann, B. & Helmchen, F. Supralinear Ca^{2+} influx into dendritic tufts of layer 2/3 neocortical pyramidal neurons *in vitro* and *in vivo*. *J. Neurosci.* **23**, 8558–8567 (2003).
81. Charpak, S., Mertz, J., Beaurepaire, E., Moreaux, L. & Delaney, K. Odor-evoked calcium signals in dendrites of rat mitral cells. *Proc. Natl Acad. Sci. USA* **98**, 1230–1234 (2001).
82. Stuart, G., Spruston, N., Sakmann, B. & Hausser, M. Action potential initiation and backpropagation in neurons of the mammalian CNS. *Trends Neurosci.* **20**, 125–131 (1997).
83. Hausselt, S. E., Euler, T., Detwiler, P. B. & Denk, W. A dendrite-autonomous mechanism for direction selectivity in retinal starburst amacrine cells. *PLoS Biol.* **5**, e185 (2007).
84. Dombeck, D. A., Khabbaz, A. N., Collman, F., Adelman, T. L. & Tank, D. W. Imaging large-scale neural activity with cellular resolution in awake, mobile mice. *Neuron* **56**, 43–57 (2007).
This was the first study to image activity in populations of neurons stained with Ca^{2+}-sensitive dye in the awake, head-fixed mouse. The mice were trained to walk on a rotating sphere while neuronal populations were simultaneously imaged.
85. Helmchen, F., Fee, M. S., Tank, D. W. & Denk, W. A miniature head-mounted two-photon microscope. High-resolution brain imaging in freely moving animals. *Neuron* **31**, 903–912 (2001).
This paper introduced a new method for imaging that provided cellular resolution in the awake, behaving rodent.
86. Flusberg, B. A., Jung, J. C., Cocker, E. D., Anderson, E. P. & Schnitzer, M. J. *In vivo* brain imaging using a portable 3.9 gram two-photon fluorescence microendoscope. *Opt. Lett.* **30**, 2272–2274 (2005).
87. Piyawattanametha, W. *et al.* Fast-scanning two-photon fluorescence imaging based on a microelectromechanical systems two- dimensional scanning mirror. *Opt. Lett.* **31**, 2018–2020 (2006).
88. Sawinski, J. & Denk, W. Miniature random-access fiber scanner for *in vivo* multiphoton imaging. *J. Appl. Phys.* **102**, 034701 (2007).
89. Adelsberger, H., Garaschuk, O. & Konnerth, A. Cortical calcium waves in resting newborn mice. *Nature Neurosci.* **8**, 988–990 (2005).
90. Murayama, M., Perez-Garci, E., Luscher, H. R. & Larkum, M. E. Fiberoptic system for recording dendritic calcium signals in layer 5 neocortical pyramidal cells in freely moving rats. *J. Neurophysiol.* **98**, 1791–1805 (2007).
91. Sobel, E. C. & Tank, D. W. *In vivo* Ca^{2+} dynamics in a cricket auditory neuron: an example of chemical computation. *Science* **263**, 823–826 (1994).
92. Single, S. & Borst, A. Dendritic integration and its role in computing image velocity. *Science* **281**, 1848–1850 (1998).
93. Haag, J., Denk, W. & Borst, A. Fly motion vision is based on Reichardt detectors regardless of the signal-to-noise ratio. *Proc. Natl Acad. Sci. USA* **101**, 16333–16338 (2004).
94. Kerr, R. *et al.* Optical imaging of calcium transients in neurons and pharyngeal muscle of *C. elegans*. *Neuron* **26**, 583–594 (2000).
95. Ng, M. *et al.* Transmission of olfactory information between three populations of neurons in the antennal lobe of the fly. *Neuron* **36**, 463–474 (2002).
96. Wang, J. W., Wong, A. M., Flores, J., Vosshall, L. B. & Axel, R. Two-photon calcium imaging reveals an odor-evoked map of activity in the fly brain. *Cell* **112**, 271–282 (2003).
97. Higashijima, S., Masino, M. A., Mandel, G. & Fetcho, J. R. Imaging neuronal activity during zebrafish behavior with a genetically encoded calcium indicator. *J. Neurophysiol.* **90**, 3986–3997 (2003).
98. Miyawaki, A. *et al.* Fluorescent indicators for Ca^{2+} based on green fluorescent proteins and calmodulin. *Nature* **388**, 882–887 (1997).
This was the first study to demonstrate that genetically encoded fluorescent proteins targeted to specific intracellular locations can be used to report intracellular changes in $[Ca^{2+}]$.
99. Tsien, R. Y. A non-disruptive technique for loading calcium buffers and indicators into cells. *Nature* **290**, 527–528 (1981).
100. Smetters, D., Majewska, A. & Yuste, R. Detecting action potentials in neuronal populations with calcium imaging. *Methods* **18**, 215–221 (1999).
101. Friedrich, R. W. & Korsching, S. I. Combinatorial and chemotopic odorant coding in the zebrafish olfactory bulb visualized by optical imaging. *Neuron* **18**, 737–752 (1997).
102. Friedrich, R. W. & Korsching, S. I. Chemotopic, combinatorial, and noncombinatorial odorant representations in the olfactory bulb revealed using a voltage-sensitive axon tracer. *J. Neurosci.* **18**, 9977–9988 (1998).
103. Sato, T. R., Gray, N. W., Mainen, Z. F. & Svoboda, K. The functional microarchitecture of the mouse barrel cortex. *PLoS Biol.* **5**, e189 (2007).
104. Sullivan, M. R., Nimmerjahn, A., Sarkisov, D. V., Helmchen, F. & Wang, S. S. *In vivo* calcium imaging of circuit activity in cerebellar cortex. *J. Neurophysiol.* **94**, 1636–1644 (2005).
105. Niell, C. M. & Smith, S. J. Functional imaging reveals rapid development of visual response properties in the zebrafish tectum. *Neuron* **45**, 941–951 (2005).
106. Wachowiak, M., Denk, W. & Friedrich, R. W. Functional organization of sensory input to the olfactory bulb glomerulus analyzed by two-photon calcium imaging. *Proc. Natl Acad. Sci. USA* **101**, 9097–9102 (2004).
107. Li, J. *et al.* Early development of functional spatial maps in the zebrafish olfactory bulb. *J. Neurosci.* **25**, 5784–5795 (2005).
108. Yaksi, E., Judkewitz, B. & Friedrich, R. W. Topological reorganization of odor representations in the olfactory bulb. *PLoS Biol.* **5**, e178 (2007).
109. Bonhoeffer, T. & Grinvald, A. Iso-orientation domains in cat visual-cortex are arranged in pinwheel-like patterns. *Nature* **353**, 429–431 (1991).
Using intrinsic optical imaging of the cat visual cortex, this study was the first to show the existence of orientation pinwheels.
110. Brecht, M., Roth, A. & Sakmann, B. Dynamic receptive fields of reconstructed pyramidal cells in layers 3 and 2 of rat somatosensory barrel cortex. *J. Physiol.* **553**, 243–265 (2003).
111. de Kock, C. P., Bruno, R. M., Spors, H. & Sakmann, B. Layer- and cell-type-specific suprathreshold stimulus representation in rat primary somatosensory cortex. *J. Physiol.* **581**, 139–154 (2007).
112. Nimmerjahn, A., Kirchhoff, F., Kerr, J. N. & Helmchen, F. Sulforhodamine 101 as a specific marker of astroglia in the neocortex *in vivo*. *Nature Methods* **1**, 31–37 (2004).
113. Delaney, K., Davison, I. & Denk, W. Odour-evoked $[Ca^{2+}]$ transients in mitral cell dendrites of frog olfactory glomeruli. *Eur. J. Neurosci.* **13**, 1658–1672 (2001).
114. Yuste, R. & Denk, W. Dendritic spines as basic functional units of neuronal integration. *Nature* **375**, 682–684 (1995).
115. Denk, W., Yuste, R., Svoboda, K. & Tank, D. W. Imaging calcium dynamics in dendritic spines. *Curr. Opin. Neurobiol.* **6**, 372–378 (1996).
116. Hasan, M. T. *et al.* Functional fluorescent Ca^{2+} indicator proteins in transgenic mice under TET control. *PLoS Biol.* **2**, e163 (2004).
117. Diez-Garcia, J. *et al.* Activation of cerebellar parallel fibers monitored in transgenic mice expressing a fluorescent Ca^{2+} indicator protein. *Eur. J. Neurosci.* **22**, 627–635 (2005).
118. Heim, N. *et al.* Improved calcium imaging in transgenic mice expressing a troponin C-based biosensor. *Nature Methods* **4**, 127–129 (2007).
119. Diez-Garcia, J., Akemann, W. & Knopfel, T. *In vivo* calcium imaging from genetically specified target cells in mouse cerebellum. *Neuroimage* **34**, 859–869 (2007).
120. Osten, P., Grinevich, V. & Cetin, A. in *Conditional Mutagenesis: An Approach to Disease Models (Handbook of Experimental Pharmacology)* (eds Feil, R. & Metzger, D.) 177–202 (Springer, Berlin, 2007).
121. Margrie, T. W. *et al.* Targeted whole-cell recordings in the mammalian brain *in vivo*. *Neuron* **39**, 911–918 (2003).
122. Euler, T., Detwiler, P. B. & Denk, W. Directionally selective calcium signals in dendrites of starburst amacrine cells. *Nature* **418**, 845–852 (2002).
123. Stuart, G. J., Dodt, H. U. & Sakmann, B. Patch-clamp recordings from the soma and dendrites of neurons in brain slices using infrared video microscopy. *Pflugers Arch.* **423**, 511–518 (1993).
124. Dittgen, T. *et al.* Lentivirus-based genetic manipulations of cortical neurons and their optical and electrophysiological monitoring *in vivo*. *Proc. Natl Acad. Sci. USA* **101**, 18206–18211 (2004).
125. Komai, S. *et al.* Postsynaptic excitability is necessary for strengthening of cortical sensory responses during experience-dependent development. *Nature Neurosci.* **9**, 1125–1133 (2006).
126. Niell, C. M., Meyer, M. P. & Smith, S. J. *In vivo* imaging of synapse formation on a growing dendritic arbor. *Nature Neurosci.* **7**, 254–260 (2004).
127. Calverley, R. K. & Jones, D. G. Contributions of dendritic spines and perforated synapses to synaptic plasticity. *Brain Res. Brain Res. Rev.* **15**, 215–249 (1990).
128. Balicegordon, R. J. & Lichtman, J. W. *In vivo* visualization of the growth of presynaptic and postsynaptic elements of neuromuscular-junctions in the mouse. *J. Neurosci.* **10**, 894–908 (1990).
129. Sanes, J. R. & Lichtman, J. W. Development of the vertebrate neuromuscular junction. *Annu. Rev. Neurosci.* **22**, 389–442 (1999).
130. Javaherian, A. & Cline, H. T. Coordinated motor neuron axon growth and neuromuscular synaptogenesis are promoted by CPG15 *in vivo*. *Neuron* **45**, 505–512 (2005).
131. Hua, J. Y., Smear, M. C., Baier, H. & Smith, S. J. Regulation of axon growth *in vivo* by activity-based competition. *Nature* **434**, 1022–1026 (2005).
132. Wu, G. Y. & Cline, H. T. Time-lapse *in vivo* imaging of the morphological development of *Xenopus* optic tectal interneurons. *J. Comp. Neurol.* **459**, 392–406 (2003).
133. Kulesa, P. M. & Fraser, S. E. Cell dynamics during somite boundary formation revealed by time-lapse analysis. *Science* **298**, 991–995 (2002).
134. Feng, G. *et al.* Roles for ephrins in positionally selective synaptogenesis between motor neurons and muscle fibers. *Neuron* **25**, 295–306 (2000).
135. Zuo, Y., Lin, A., Chang, P. & Gan, W. B. Development of long-term dendritic spine stability in diverse regions of cerebral cortex. *Neuron* **46**, 181–189 (2005).
136. Holtmaat, A., Wilbrecht, L., Knott, G. W., Welker, E. & Svoboda, K. Experience-dependent and cell-type-specific spine growth in the neocortex. *Nature* **441**, 979–983 (2006).
137. Nimmerjahn, A., Kirchhoff, F. & Helmchen, F. Resting microglial cells are highly dynamic surveillants of brain parenchyma *in vivo*. *Science* **308**, 1314–1318 (2005).
138. De Paola, V. *et al.* Cell type-specific structural plasticity of axonal branches and boutons in the adult neocortex. *Neuron* **49**, 861–875 (2006).

139. Mizrahi, A. Dendritic development and plasticity of adult-born neurons in the mouse olfactory bulb. *Nature Neurosci.* **10**, 444–452 (2007).
140. Theer, P., Hasan, M. T. & Denk, W. Two-photon imaging to a depth of 1000 µm in living brains by use of a Ti:Al_2O_3 regenerative amplifier. *Opt. Lett.* **28**, 1022–1024 (2003).
141. Theer, P. & Denk, W. On the fundamental imaging-depth limit in two-photon microscopy. *J. Opt. Soc. Am. A Opt. Image Sci. Vis.* **23**, 3139–3149 (2006).
This paper provides a thorough description, both theoretical and experimental, of the physical properties of two-photon imaging in light scattering media, with a focus on the imaging-depth limit.
142. Feierabend, M., Ruckel, M. & Denk, W. Coherence-gated wave-front sensing in strongly scattering samples. *Opt. Lett.* **29**, 2255–2257 (2004).
143. Rueckel, M., Mack-Bucher, J. A. & Denk, W. Adaptive wavefront correction in two-photon microscopy using coherence-gated wavefront sensing. *Proc. Natl Acad. Sci. USA* **103**, 17137–17142 (2006).
This study showed how both imaging resolution and signal size were improved by measuring beam wavefront distortions and compensating for these distortions using adaptive optics. This technology will be of great benefit to imaging in preparations in which both intact dura and skull are required.
144. Kralik, J. D. *et al.* Techniques for long-term multisite neuronal ensemble recordings in behaving animals. *Methods* **25**, 121–150 (2001).
145. Mehta, A. D., Jung, J. C., Flusberg, B. A. & Schnitzer, M. J. Fiber optic *in vivo* imaging in the mammalian nervous system. *Curr. Opin. Neurobiol.* **14**, 617–628 (2004).
146. Jung, J. C., Mehta, A. D., Aksay, E., Stepnoski, R. & Schnitzer, M. J. *In vivo* mammalian brain imaging using one- and two-photon fluorescence microendoscopy. *J. Neurophysiol.* **92**, 3121–3133 (2004).
147. Zucker, R. S. & Regehr, W. G. Short-term synaptic plasticity. *Annu. Rev. Physiol.* **64**, 355–405 (2002).
148. Fan, G. Y. *et al.* Video-rate scanning two-photon excitation fluorescence microscopy and ratio imaging with cameleons. *Biophys. J.* **76**, 2412–2420 (1999).
149. Lechleiter, J. D., Lin, D. T. & Sieneart, I. Multi-photon laser scanning microscopy using an acoustic optical deflector. *Biophys. J.* **83**, 2292–2299 (2002).
150. Vucinic, D. & Sejnowski, T. A compact multiphoton 3D imaging system for recording fast neuronal activity. *PLoS ONE* **2**, e699 (2007).
151. Gobel, W., Kampa, B. M. & Helmchen, F. Imaging cellular network dynamics in three dimensions using fast 3D laser scanning. *Nature Methods* **4**, 73–79 (2007).
152. Livet, J. *et al.* Transgenic strategies for combinatorial expression of fluorescent proteins in the nervous system. *Nature* **450**, 56–62 (2007).
153. Levene, M. J., Dombeck, D. A., Kasischke, K. A., Molloy, R. P. & Webb, W. W. *In vivo* multiphoton microscopy of deep brain tissue. *J. Neurophysiol.* **91**, 1908–1912 (2004).
154. Gobel, W., Kerr, J. N., Nimmerjahn, A. & Helmchen, F. Miniaturized two-photon microscope based on a flexible coherent fiber bundle and a gradient-index lens objective. *Opt. Lett.* **29**, 2521–2523 (2004).
155. Yaksi, E. & Friedrich, R. W. Reconstruction of firing rate changes across neuronal populations by temporally deconvolved Ca^{2+} imaging. *Nature Methods* **3**, 377–383 (2006).
This study describes a deconvolution-based method for estimating spike firing rates in neuronal populations bulk-loaded with Ca^{2+}-indicator in the zebrafish tectum.
156. Takano, T. *et al.* Astrocyte-mediated control of cerebral blood flow. *Nature Neurosci.* **9**, 260–267 (2006).
157. Winship, I. R., Plaa, N. & Murphy, T. H. Rapid astrocyte calcium signals correlate with neuronal activity and onset of the hemodynamic response *in vivo*. *J. Neurosci.* **27**, 6268–6272 (2007).
158. Takano, T., Han, X., Deane, R., Zlokovic, B. & Nedergaard, M. Two-photon imaging of astrocytic Ca^{2+} signaling and the microvasculature in experimental mice models of Alzheimer's disease. *Ann. NY Acad. Sci.* **1097**, 40–50 (2007).
159. Zipfel, W. R. *et al.* Live tissue intrinsic emission microscopy using multiphoton-excited native fluorescence and second harmonic generation. *Proc. Natl Acad. Sci. USA* **100**, 7075–7080 (2003).
160. Misgeld, T. & Kerschensteiner, M. *In vivo* imaging of the diseased nervous system. *Nature Rev. Neurosci.* **7**, 449–463 (2006).
161. Kovacevic, N. *et al.* A three-dimensional MRI atlas of the mouse brain with estimates of the average and variability. *Cereb. Cortex* **15**, 639–645 (2005).
162. Gobel, W. & Helmchen, F. New angles on neuronal dendrites *in vivo*. *J. Neurophysiol.* **98**, 3770–3779 (2007).

Competing interests statement
The authors declare competing financial interests: see web version for details.

FURTHER INFORMATION
Winfried Denk's homepage: http://www.mpimf-heidelberg.mpg.de/abteilungen/biomedizinischeOptik/index.html
Jason Kerr's homepage: http://www.kyb.tuebingen.mpg.de/kerrgroup/index.html

ALL LINKS ARE ACTIVE IN THE ONLINE PDF